



1        **Structure and evolution of the drainage system of a Himalayan debris-**  
2                    **covered glacier, and its relationship with patterns of mass loss**

3        Douglas I. Benn<sup>1</sup>, Sarah Thompson<sup>2</sup>, Jason Gulley<sup>3</sup>, Jordan Mertes<sup>4</sup>, Adrian Luckman<sup>2</sup> and  
4        Lindsey Nicholson<sup>5</sup>

6        <sup>1</sup> *School of Geography and Sustainable Development, University of St Andrews, UK*

7        <sup>2</sup> *Department of Geography, Swansea University, Swansea, UK*

8        <sup>3</sup> *School of Geosciences, University of South Florida, FL, USA*

9        <sup>4</sup> *Department of Geological and Mining Engineering and Sciences, Michigan Tech, MI, USA*

10       <sup>5</sup> *Institute for Atmospheric and Cryospheric Sciences, University of Innsbruck, Austria*

12       **Abstract**

13       This paper provides the first synoptic view of the drainage system of a Himalayan debris-  
14       covered glacier and its evolution through time, based on speleological exploration and  
15       satellite image analysis of Ngozumpa Glacier, Nepal. The drainage system has several linked  
16       components: 1) a seasonal subglacial drainage system below the upper ablation zone; 2)  
17       supraglacial channels allowing efficient meltwater transport across parts of the upper ablation  
18       zone; 3) sub-marginal channels, allowing long-distance transport of meltwater; 4) perched  
19       lakes, which intermittently store meltwater prior to evacuation via the englacial drainage  
20       system; 5) englacial cut-and-closure conduits, which may undergo repeated cycles of  
21       abandonment and reactivation; 6) a 'base-level' lake system (Spillway Lake) dammed behind  
22       the terminal moraine. The distribution and relative importance of these elements has evolved  
23       through time, in response to sustained negative mass balance. The area occupied by perched  
24       lakes has expanded upglacier at the expense of supraglacial channels, and Spillway Lake has  
25       grown as more of the glacier surface ablates to base level. Subsurface processes play a  
26       governing role in creating, maintaining and shutting down exposures of ice at the glacier



27 surface, with a major impact on spatial patterns and rates of surface mass loss. Comparison of  
28 our results with observations on other glaciers indicate that englacial drainage systems play a  
29 key role in the response of debris-covered glaciers to sustained periods of negative mass  
30 balance.

31

## 32 **1. Introduction**

33 Debris-covered glaciers in many parts of the Himalaya have undergone significant surface  
34 lowering in recent decades, with net losses of several tens of metres since the 1970s (Bolch et  
35 al., 2008a, 2011; Kääb et al., 2012). Glacier thinning and reduced surface gradients have  
36 resulted in lower driving stresses and ice velocities, and large parts of many glaciers are now  
37 stagnant or nearly so (Bolch et al., 2008b; Quincey et al., 2009). These morphological and  
38 dynamic changes have encouraged formation of supraglacial lakes and increased water  
39 storage within glacial hydrological systems (Reynolds, 2000; Quincey et al., 2007; Benn et  
40 al., 2012). Where lakes form behind dams of moraine and ice, volumes of stored water can be  
41 as high as  $10^8 \text{ m}^3$ , in some cases posing considerable risk of glacier lake outburst floods  
42 (GLOFs) (Yamada, 1998; Richardson and Reynolds, 2000; Kattelman, 2003).

43

44 Several studies have shown that the development and enlargement of englacial conduits play  
45 an important role in the evolution of debris-covered glaciers during periods of negative mass  
46 balance (e.g. Clayton, 1964; Kirkbride, 1993; Krüger, 1994; Benn et al., 2001, 2009, 2012;  
47 Gulley and Benn, 2007; Thompson et al., 2016). The collapse of conduit roofs can expose  
48 areas of bare ice at the glacier surface, locally increasing ablation rates. Additionally, areas of  
49 subsidence associated with englacial conduits create closed hollows (dolines) that can evolve  
50 into supraglacial ponds and lakes, further increasing ice losses by calving. Conversely,  
51 supraglacial lakes can drain if a connection is made with the englacial drainage system,  
52 provided the lake is elevated above hydrological base level ('perched lakes'; Benn et al.,



53 2001). Drainage of relatively warm lake waters through the glacier leads to conduit  
54 enlargement, which in turn increases the likelihood of roof collapse, surface subsidence and  
55 ultimately new lake formation (Sakai et al., 2000; Miles et al., 2015). Because ablation rates  
56 around supraglacial lake margins are typically one or two orders of magnitude higher than  
57 that under continuous surface debris, lakes contribute disproportionately to overall rates of  
58 glacier ablation (Sakai et al., 1998, 2000, 2009; Thompson et al., 2016). By controlling the  
59 location and frequency of surface subsidence and lake drainage events, englacial conduits  
60 strongly influence overall ablation rates, and the volume of water that can be stored in and on  
61 the glacier (Benn et al., 2012).

62

63 Speleological investigations in debris-covered glaciers in the Khumbu Himal have  
64 demonstrated that englacial conduits can form by three processes: 1) 'cut and closure' or the  
65 incision of supraglacial stream beds followed by roof closure; 2) hydrologically assisted  
66 crevasse propagation, or hydrofracturing, which may route water to glacier beds; and 3)  
67 exploitation of secondary permeability in the ice (Gulley et al., 2009a, b; Benn et al., 2012).  
68 The relative importance of these processes in the development of glacial drainage systems,  
69 however, has not been investigated in detail. Furthermore, there are no data on the large-scale  
70 structure of englacial and subglacial glacial drainage systems in the Himalaya, or how they  
71 evolve during periods of negative mass balance. In this paper, we investigate the origin,  
72 configuration and evolution of the drainage system of Ngozumpa Glacier, using three  
73 complementary methods. First, speleological surveys of englacial conduits are used to  
74 provide a detailed understanding of their formation and evolution. Second, historical satellite  
75 imagery and high-resolution digital elevation models (DEMs) are used to identify past and  
76 present drainage pathways, glacier-wide patterns of surface water storage and release, and  
77 regions of subsidence. Finally, feature tracking on TerraSAR-X imagery is used to detect  
78 regions of the glacier subject to seasonal velocity fluctuations, as a proxy for variations in



79 subglacial water storage. Taken together, these methods provide the first synoptic view of the  
80 drainage system of a large Himalayan debris-covered glacier, and its influence on glacier  
81 response to recent warming.

82

## 83 **2. Study area and methods**

84 Ngozumpa Glacier is located in the upper Dudh Kosi catchment, Khumbu Himal, Nepal (Fig.  
85 1). It has three confluent branches: a western (W) branch flowing from the flanks of Cho Oyu  
86 (8188 m); a north-eastern (NE) branch originating below Gyachung Kang (7922 m); and an  
87 eastern (E) branch (Gaunara Glacier) nourished below a cirque of 6000 m peaks. The NE and  
88 E branches are no longer dynamically connected to the main trunk, which is fed solely by the  
89 W branch (Thompson et al., 2016). The equilibrium line altitude (ELA) is not well known.  
90 Google Earth images from 3 November 2009 (after the end of the ablation season) and 9 June  
91 2010 (at the beginning of the monsoon accumulation season) show bare ice up to ~5700 m  
92 above sea level (a.s.l.) on all three branches, and this value is adopted as an approximate  
93 value of the ELA.

94

95 The lower ablation zone of the glacier is stagnant, with little or no detectable motion on most  
96 of the E branch, or on the main trunk for ~7 km upglacier of the terminus (Bolch et al.,  
97 2008b; Quincey et al., 2009; Thompson et al., 2016). The lowermost 15 km of the glacier  
98 (below ~5250 m a.s.l.) is almost completely mantled with supraglacial debris. The debris  
99 cover thickens downglacier, reaching  $1.80 \pm 1.21$  m near the terminus (Nicholson, 2004;  
100 Nicholson and Benn, 2012). In common with other large debris-covered glaciers in the  
101 region, Ngozumpa Glacier has undergone significant surface lowering in recent decades, and  
102 the glacier surface now lies >100 m below the crestlines of the late Holocene lateral moraines  
103 (Bolch et al., 2008a, 2011).

104





105 The lower tongue of the glacier has a highly irregular surface, with numerous closed basins  
106 separated by mounds, ridges and plateaux with a relative relief of ~50 m (Fig. 2). Most basins  
107 contain supraglacial ponds and lakes, which typically persist for a few years before draining  
108 (Benn et al., 2001; 2009, 2012; Gulley and Benn, 2007). Near the terminus of Ngozumpa  
109 Glacier, a system of lakes is ponded behind the terminal moraine (informally named Spillway  
110 Lake; Fig. 1). This lake system increased in area by around 10% per year from the early  
111 1990s until 2009, but between 2009 and 2015 experienced a reduction of area and volume as  
112 a result of lake level lowering and redistribution of sediment (Thompson et al., 2012, 2016;  
113 Mertes et al., 2016). This hiatus is likely to be temporary and continued growth of the lake is  
114 expected in the coming years, as has been the case with other ‘base-level lakes’ in the region  
115 (Sakai et al., 2009).

116

117 We surveyed 2.3 km of englacial passages in Ngozumpa Glacier, using standard  
118 speleological techniques modified for glacier caves (Gulley and Benn, 2007). Conduit  
119 entrances were identified during systematic traverses of the glacier surfaces. Within each  
120 conduit, networks of survey lines were established by measuring the distance, azimuth and  
121 inclination between successive marked stations using a Leica Distomat laser rangefinder and  
122 a Brunton Sightmaster compass and inclinometer. Scaled drawings of passages in plan,  
123 profile and cross-section were then rendered *in situ*, and include observations of  
124 glaciostructural and stratigraphic features exposed in passage walls, thereby allowing the  
125 origin and evolution of conduits to be reconstructed in detail. In this paper, we focus on five  
126 conduits, which exemplify different stages of conduit formation, abandonment and  
127 reactivation. Three of the conduits have been previously described by Gulley and Benn  
128 (2007), but in this paper we revise our interpretation of their origin in some important  
129 respects. Some of the conduits drained water from or fed water into supraglacial lakes, and in



130 some cases it was possible to relate phases of conduit development to specific lake filling or  
131 drainage events, identified in satellite images.

132

133 A range of optical imagery was used to map indicators of the large-scale structure of the  
134 drainage system (Table 1). The location of supraglacial channels and ephemeral supraglacial  
135 ponds were mapped using declassified Corona KH-4 imagery from 1965, Landsat 5 TM  
136 (2009), GeoEye-1 (9 June 2010 and 23 December 2012) and WorldView-3 (5 January 2015)  
137 imagery. The Corona and Landsat imagery was not co-registered or orthorectified beyond the  
138 standard terrain correction of the product, and was used to identify the presence / absence of  
139 larger lakes or channels and not to quantify rates of change.

140

141 Geo-Eye-1 imagery from June 2010 and December 2012, and Worldview-3 imagery from  
142 January 2015 were acquired for a region covering 17.4 km<sup>2</sup> of the ablation area of the glacier.  
143 Three stereoscopic DEMs of 1 m resolution were constructed from the stereo multispectral  
144 imagery using the PCI Geomatica Software Package, and used to determine spatial patterns  
145 of elevation change. The construction and correction of the DEMs is discussed in detail in  
146 Thompson et al. (2016).

147

148 The 2010 DEM was used to define the extent of individual surface drainage basins on the  
149 glacier surface. This was achieved by identifying surface elevation contours that entirely  
150 surround other contours of a lesser height. Each supraglacial catchment was then defined by  
151 the crestlines of ridges that separate the closed basins. Initially, we used 2 m contours but  
152 these produced a large number of very small 'basins', due to the high roughness of the  
153 bouldery glacier surface. Subsequently, we used 5 m contours that yielded a set of closed  
154 basins that closely matched the location of ephemeral supraglacial ponds and lakes on the



155 glacier surface. The extent of many basins changed between 2010 and 2015 due to ice-cliff  
156 backwasting, although all basins persisted through the period covered by the DEMs.

157

158 Glacier surface velocities were derived using feature tracking between synthetic aperture  
159 radar images acquired by the TerraSAR-X satellite on 19 September 2014, 18 and 29 January  
160 2015 and 5 January 2016. Feature tracking was done using the method of Luckman et al.  
161 (2007), which searches for a maximum correlation between evenly spaced subsets (patches)  
162 of each image giving the displacement of glacier surface features which are converted to  
163 speed using time delay between images. Image patches were ~400 m x 400 m in size and  
164 sampled every 40 m producing a spatial resolution of between 40 and 400 m depending on  
165 feature density. Based on feature matching precise to one pixel (2 m), precision of the  
166 measured velocities is 0.006 m day<sup>-1</sup> over the annual (341 day) period and 0.018 m day<sup>-1</sup> over  
167 the winter (111 day) period.

168

### 169 **3. Mechanisms of englacial conduit formation**

170 To provide a comprehensive view of processes of englacial conduit formation on the glacier,  
171 we describe two sites in detail (NG-04 and NG-05), then briefly describe and reinterpret three  
172 previously published sites (NG-01, NG-02 and NG-03; Gulley and Benn, 2007).

173

#### 174 *3.1 NG-04*

175 *Description:* Conduit NG-04 (27°57'24"N, 86°41'55" E; 4805 m a.s.l.) was surveyed in  
176 November 2009, and consisted of a main passage (A; Fig. 3) and two shorter side-passages  
177 (B and C) leading off to the west. The main passage extended from a large hollow on the  
178 glacier surface (Basin C-63 on Fig. 9a) for a distance of at least 473 m (Fig. 2e), where the  
179 survey was discontinued due to deep standing water on the cave floor. Side-passage B also  
180 connected with a basin on the glacier surface (Basin W-6, Fig. 9b). Side-passage C was at



181 least 25 m long, but was not surveyed beyond this distance due to the evident instability of  
182 the highly fractured walls.

183

184 The main passage consisted of an upper level with a flat or gently inclined floor, and a lower  
185 narrow incised canyon. The passage was highly sinuous, with a sinuosity in the surveyed  
186 reach of 5.52. Near A4 (Fig. 3), there was a tight cutoff meander loop off the main passage  
187 (Fig. 4a). The base of the abandoned loop had a flat floor and lacked the incised lower level  
188 that was present elsewhere in the system. The upper floor level could also be traced along the  
189 walls of side passages B and C, which we interpret as twin remnants of a second meander  
190 cutoff. The floor of the upper level sloped gently downward from A1 to A14, rose from there  
191 to between A18 and A19, after which it descended once more. Sandy bedforms on the floor  
192 and scallops on the ice walls of this upper level indicate that water flow was from A1 towards  
193 A21.

194

195 Passage morphology in the upper level was very variable, including tubular, box-shaped,  
196 triangular and irregular sections (Figs. 3 & 4b-d). Throughout most of the system, planar  
197 structures were visible in the ceiling or walls of the upper level, running parallel to the  
198 passage axis with variable inclination. The structures took the form of: (1) ‘sutures’ at the  
199 line of contact between opposing walls (S: Fig. 3; Fig. 4b, c), (2) intermittent narrow voids  
200 (V: Fig. 3; Fig. 4c), and (3) bands of sorted sand or gravel a few cm thick (SB: Fig. 3; Fig.  
201 4d). Some of the voids increased in width inward, in some cases opening out into gaps tens of  
202 cm across. In some places, bands of sorted sediment could be traced laterally into open voids  
203 or sutures. At several points along the main passage, a pair of planar structures occurred on  
204 opposite walls of the passage. Side-passage B had a narrow, meandering seam of dirty ice  
205 running along its ceiling, and in Passage C the walls tapered upward to meet at a ceiling  
206 suture.



207

208 The floor of the incised lower level in both parts of the main passage sloped down towards  
209 side passages B and C (arrows, Fig. 3). A pair of incised channels was confluent at C1,  
210 whereas a single incised channel was present in passage B, where its lower (western) end was  
211 blocked by an accumulation of ice and debris.

212

213 *Interpretation:* The partially debris-filled structures in the walls and ceiling of the upper level  
214 are closely similar to many examples of canyon sutures we have observed in cut-and-closure  
215 conduits in the Himalaya and Svalbard, marking the planes of closure where former passage  
216 walls have been brought together by ice creep and/or blocked by ice and debris (cf. Gulley et  
217 al., 2009a, b). Cut-and-closure conduits are typically highly sinuous and have variable cross  
218 sectional morphologies, ranging from simple *plugged canyons* (incised channels with roofs of  
219 névé), to *sutured canyons* (partially or completely closed by ice creep), *horizontal slots*  
220 (formed by lateral channel migration followed by roof closure), and *tubular passages* (where  
221 passage re-enlargement has occurred under pipe-full (phreatic) conditions (Gulley et al.,  
222 2009b). The tubular morphology of the upper passage in NG-04, combined with the sutures,  
223 voids and sediment bands in the walls and ceiling indicates that the passage has been re-  
224 enlarged under pipe-full conditions following an episode of almost complete closure. For  
225 example, the sub-horizontal bands of sorted sand on both conduit walls between A15 and  
226 A18 (Fig. 3d) suggest complete suturing of a low, wide reach (horizontal slot) prior to  
227 formation of the surveyed passage.

228

229 The tubular and box-shaped cross-profiles and undulating long-profile of the upper passage  
230 are consistent with fluvial erosion under pipe-full or phreatic conditions (cf. Gulley et al.,  
231 2009b). This contrasts with the canyon-like form and consistent down-flow slope of channels  
232 incised under atmospheric (vadose) conditions, typical of simple cut-and-closure conduits.



233 The dimensions of the upper passage (typically 2 m high and 3 m wide) are consistent with  
234 high discharges. We conclude that the upper passage formed when water draining from a  
235 supraglacial lake in Basin C-63 exploited the remnants of an abandoned cut-and-closure  
236 conduit (Fig. 2e).

237

238 Following formation of the upper passage, the lower level was incised under vadose (non  
239 pipe-full) conditions when the system accessed a new local base level via side-passages B  
240 and C. We infer that this occurred when the cutoff meander loop between B1 and C2 was  
241 exposed by ice-cliff retreat in Basin W-6. Water flow between A1 and B2 continued in the  
242 same direction as before, but between A14 and A21 flow was reversed and discharge much  
243 reduced.

244

245 Evolution of conduit NG-04 can be summarized as follows: 1) a cut-and-closure conduit was  
246 formed by incision of a supraglacial stream; 2) this conduit was abandoned and almost  
247 completely closed, presumably after it lost all or most of its source of recharge following  
248 downwasting of the overlying glacier surface; 3) the conduit remnants were exploited and  
249 enlarged by water draining from a supraglacial pond in Basin C-63; and 4) surface ablation in  
250 Basin W-6 broke into the conduit, creating a new base level and initiating floor incision. This  
251 remarkable cave illustrates how relict drainage systems can be reactivated when connected to  
252 new sources of recharge, and demonstrates how patterns of drainage can change dramatically  
253 within a single system in response to changing surface topography.

254

### 255 3.2 NG-05

256 *Description:* In December 2009 a conduit portal was exposed in an ice cliff at the margin of  
257 Spillway Lake (27°56'36" N, 86°42'46" E, 4670 m a. s. l.). This portal was one of the two  
258 main efflux points that carried water into the lake from upglacier (Thompson et al., 2016).



259 Access to the conduit could be gained via the frozen lake surface. However, the lake ice was  
260 broken up each morning by debris falling from the melting glacier surface above, severely  
261 limiting the time available for survey. Consequently, only a short section could be mapped  
262 (Fig. 5). The conduit had two main levels, separated by a narrow, partially ice-filled canyon.  
263 The floor of the lower part was at lake level, and that of the upper level was 4.8 m higher,  
264 close to the summer monsoon level of the lake, as indicated by shorelines exposed around the  
265 lake margins. Several notches on the passage walls recorded intermediate water levels. The  
266 ice cliff above the upper level was obscured by a mass of icicles, but observations inside the  
267 cave showed that the roof tapered up into a narrow, debris band or suture (Fig. 6a).

268

269 *Interpretation:* Although short, this passage is important for understanding the drainage  
270 system of Ngozumpa Glacier. The debris band and suture in the roof indicates that, like NG-  
271 04, the passage formed by a process of channel incision and roof closure. Additionally, the  
272 passage is graded to the seasonally fluctuating surface of Spillway Lake. We therefore  
273 conclude that the main drainage on the eastern side of the glacier consists of a cut-and-  
274 closure conduit graded to the hydrologic base level of the glacier. For several km upglacier of  
275 the portal, the debris-covered ice surface is highly irregular and broken into numerous closed  
276 basins, implying that the conduit evolved from a surface stream that predates significant  
277 downwasting of the glacier. The significance of these conclusions will be discussed later in  
278 the paper.

279

### 280 3.3 NG-01, 02 and 03

281 *Description:* NG-01, NG-02 and NG-03 were mapped in December 2005, and described by  
282 Gulley and Benn (2007) (Fig. 2e). NG-01 had carried water southward into a large basin on  
283 the glacier surface (Basin C-25, Fig. 9a), whereas NG-02 drained water southward out of the  
284 basin. NG-01 (27°57'58" N, 86°41'50" E) was a sinuous canyon passage with three main



285 levels. Debris bands cropped out in the walls of the uppermost level throughout its length,  
286 either at the lateral margins of the passage or in the roof (Fig. 6b). The mid-level had a sub-  
287 horizontal floor, into which the canyon linking to the lower level had been incised (Fig. 6c).  
288 NG-02 (27°57'55" N, 86°41'51" E) was a sinuous canyon passage on two levels, extending in  
289 a southwesterly direction from the basin. The upper level had a circular cross profile, and an  
290 incised canyon beneath formed the lower level. A suture and debris band was exposed along  
291 the entire length of the ceiling of the upper passage, mirroring the planform of the passage  
292 (Fig. 6d). The lower level was an asymmetric flat-floored passage with a series of sills along  
293 the margins. NG-03 (27°57'52" N, 86°42'02" E) consisted of a single passage graded to a  
294 supraglacial pond in Basin E-19 (Fig. 2). Passage morphology changed from a low, wide  
295 semi-elliptical cross-section to a more complex form with an elliptical upper section  
296 separated by a narrow neck from a lower A-shaped section. At the top of the canyon, the  
297 ceiling narrowed to a narrow slot, terminating in a band of coarse, unfrozen sandy debris.

298

299 *Interpretation:* For much of their length, all three conduits follow the trend of debris bands in  
300 the walls or roof, leading Gulley and Benn (2007) to conclude that all were structurally  
301 controlled. The debris bands were originally interpreted as debris-filled crevasse traces that  
302 had been deformed during advection downglacier. When the original work was conducted,  
303 the cut-and-closure model had not been developed, and we had yet to learn how to recognize  
304 the diverse forms such conduits can take, especially in the later stages of their development.  
305 It is now apparent that these conduits have all the hallmarks of cut and closure conduits. The  
306 continuity and sinuous planform of the debris bands is consistent with formation by the  
307 closure of incised canyons, rather than crevasse fills that had been deformed by ice flow.  
308 Crevasses in the upper part of the glacier ablation area tend to be short, discontinuous and  
309 oriented transverse to flow, unlike the observed debris bands in the conduit roofs, and ice





310 deformation is unlikely to be capable of generating the highly sinuous patterns observed  
311 within the conduit debris bands.

312

313 We therefore reinterpret NG-01 – 03 as cut-and-closure conduits that have undergone cycles  
314 of incision, abandonment, partial closure and later reactivation in response to fluctuating  
315 patterns of recharge on the glacier surface. The circular and elliptical cross profiles observed  
316 in NG-02 and NG-03 are consistent with phases of phreatic passage enlargement, analogous  
317 to that in NG-04. Abandoned, incompletely closed conduits create hydraulically efficient  
318 flow paths, which can be readily exploited and enlarged when surface ablation brings them  
319 into contact with new sources of recharge.

320

#### 321 **4. Drainage system structure**

322 In this section, we present evidence for the large-scale structure of the drainage system and  
323 patterns of water storage and release, using X-band radar and optical satellite imagery and  
324 high resolution DEMs from 2010, 2012 and 2015.

325

##### 326 *4.1 Subglacial drainage system*

327 *Observations:* Direct observation of the subglacial drainage system was not possible. Instead,  
328 we use seasonal fluctuations in glacier surface velocity to infer areas subject to variable  
329 subglacial water storage. Mean daily ice velocities of the glacier between 29 January 2015  
330 and 5 January 2016 are shown in Figure 7a. There is no detectable motion on the main trunk  
331 within ~6 km of the terminus or on the lowermost 6 km of the E branch. The W branch is the  
332 most active, with velocities of  $\sim 0.16 \text{ m day}^{-1}$  ( $\sim 60 \text{ m yr}^{-1}$ ) at 5300 m a.s.l., declining to near  
333 zero at 4900 m. The NE branch is slower, although velocities in its upper part could not be  
334 determined due to image 'lay-over' in steep terrain. The active part of the NE branch does not  
335 extend as far down as the confluence with the W branch, and a strip of stagnant ice  $\sim 100$  -



336 200 m wide extends ~3 km down the eastern side of the main trunk from the confluence  
337 zone. Thus, neither the E nor the NE branch is dynamically connected to the main trunk.

338

339 Evidence for seasonal velocity fluctuations is shown in Fig. 7b, which shows mean daily  
340 velocities between 29 January 2015 and 5 January 2016 (341 days) minus mean daily  
341 velocities from 19 September 2014 to 18 January 2015 (111 days). Meteorological data from  
342 the Pyramid Weather Station, at 5050 m a.s.l. c. 12 km east of Ngozumpa Glacier (available  
343 through the Ev-K2-CNR SHARE program), indicate that air temperatures were consistently  
344 below freezing between the 25th of September 2014 and the 28th of May 2015, defining a  
345 minimum winter period for the upper ablation zone. The 111 day interval lies almost entirely  
346 within the winter period but is less than half of its total duration, so Figure 7b yields  
347 minimum values for a summer speed-up on the glacier. Most of the active parts of the glacier  
348 exhibit some speed-up, although it is much more pronounced in some areas than others. On  
349 the W branch, the greatest speed-up (by  $\sim 0.015$  m day<sup>-1</sup> or  $\sim 10\%$ ) occurs above the  
350 confluence with the NE branch. Areas of lesser speed-up also occur on the main trunk below  
351 this point, although these are discontinuous and may be artifacts. Only the northern side of  
352 the NE branch is affected by a seasonal speed-up. This area coincides with the tongue of  
353 clean ice that descends through the icefall below Gyachung Kang (Fig. 1). Patchy areas of  
354 apparent speed-up and slow-down occur elsewhere on the NE branch but may be artifacts. A  
355 small speed-up also affects the active part of the E branch, above 5350 m a.s.l.

356

357 *Interpretation:* The seasonal variations in ice velocities in the upper ablation zone are too  
358 large to be explained by changes in ice creep rates, and are interpreted as variations in basal  
359 motion (sliding and/or subglacial till deformation) in response to changing subglacial water  
360 storage. This interpretation is supported by the spatial distribution of areas affected by the  
361 seasonal speed-up, which coincide with, or occur downglacier of, heavily crevassed ice.



362 Much of the upper ablation area of Ngozumpa Glacier consists of icefalls with surface  
363 gradients up to  $30^\circ$  (a, Fig. 8), and fields of transverse crevasses occur across the entire width  
364 of the W branch down to an elevation of 5150 m (b). In contrast, crevasses are much less  
365 widespread in the ablation zone of the NE branch, and occur only in the upper part of the  
366 tongue of clean ice that descends from Gyachung Kang (c). Crevasses are almost absent on  
367 the debris-covered part (d), which originates in two relatively low-altitude cirques. Fields of  
368 transverse crevasses occur in the upper basin of the E branch, above  $\sim 5400$  m. Crevasses  
369 allow meltwater to be routed rapidly to the bed, and the existence of multiple recharge points  
370 will encourage development of a distributed drainage system following the onset of the  
371 monsoon ablation season. The lack of a clear seasonal velocity response on the lowermost 10  
372 km of the glacier suggests that subglacial water is transported along the main trunk in  
373 efficient conduits.

374

#### 375 *4.2 Supraglacial channels*

376 *Observations:* Supraglacial stream networks are visible below the crevassed zones on all  
377 three branches of the glacier. The most extensive network occurs on the tongue of clean ice  
378 on the NE branch, where a set of sub-parallel channels descends from  $\sim 5180$  m to the  
379 junction with the W branch at  $\sim 4990$  m (Fig. 2b, c). There are several discontinuous  
380 supraglacial channels on the W branch between 5220 m and 5120 m a.s.l., including one  
381 along the eastern margin of the glacier. Supraglacial channels occur on both flanks of the E  
382 branch below  $\sim 5100$  m a.s.l. The channels converge at the junction with the main trunk, and  
383 after flowing over the glacier surface for several hundred metres the combined stream sinks  
384 in a large hollow that is intermittently filled with water. Patterns of water storage in this  
385 hollow are discussed in Section 4.4.

386



387 *Interpretation:* Perennial supraglacial channels can only persist if the annual amount of  
388 channel incision exceeds the amount of surface lowering of the adjacent ice (Gulley et al.,  
389 2009b). The rate at which ice-floored channels incise is controlled by viscous heat dissipation  
390 associated with turbulent flow, and increases with discharge and surface slope (Fountain and  
391 Walder, 1998; Jarosch and Gudmundsson, 2012). Because supraglacial stream discharge is a  
392 function of surface melt rate and melt area, significant channel incision requires large  
393 catchment areas. Therefore, incised surface channels tend to occur only where potential  
394 catchments are not fragmented by crevasses or hummocky surface topography (Fig. 2). At  
395 present, these conditions are met in relatively limited areas of Ngozumpa Glacier, below  
396 crevassed areas and above hummocky debris-covered areas.

397

#### 398 *4.3 Hummocky debris-covered areas and perched lakes*

399 *Observations:* Most of the lower ablation zone of the glacier (below ~5000 m) consists of  
400 hummocky debris-covered topography. In this zone, the glacier surface is broken up into  
401 numerous closed depressions, each of which forms a distinct drainage basin (Fig. 2d, e). Not  
402 including the Spillway Lake basin that drains externally, in 2010 there were 111 surface  
403 basins in the hummocky debris-covered zone (Fig. 9). The basins along the east and west  
404 margins of the glacier form a series of depressions within almost continuous lateral troughs,  
405 and are considered in Section 4.4. Here, we focus on the basins in the central part of the  
406 glacier (C1 - C69; Fig. 9a) and the terminal zone (T1 - 6, Fig. 9b).

407

408 Of the 70 basins in the central part of the glacier, 56 (80%) contained ponds or lakes in at  
409 least one of the three years covered by the Geo-Eye and Worldview imagery. Fifteen of the  
410 42 lakes present in 2010 (36%) had disappeared by 2012 or 2015, whereas 14 basins that  
411 were empty in 2010 contained lakes in one or more of the later years. Almost all of the  
412 remainder underwent partial drainage and /or refilling. In contrast, the 5 lakes in the terminal



413 zone of the glacier (below Spillway Lake) exhibited great stability. Four showed no  
414 significant change in area between 2010 and 2015, while the other showed an increase in  
415 area.

416

417 *Interpretation:* Observations on and below the glacier surface show that drainage of perched  
418 lakes occurs when part of the floor is brought into contact with permeable structures in the  
419 ice (Benn et al., 2001; Gulley and Benn, 2007). The characteristics of NG-01 - 05 (which all  
420 occur within the hummocky debris-covered zone) show that relict cut-and-closure conduits  
421 are the dominant cause of secondary permeability in the glacier, providing pre-existing lines  
422 of weakness along which perched lakes can drain.

423

424 The spatial extent and high temporal frequency of perched lake drainage events on the glacier  
425 (Fig. 9a) imply a high density of relict conduits within the ice. A rough estimate can be  
426 obtained by dividing the number of complete and partial drainage events (35) by the total  
427 area of basins in the central part of the glacier (4.62 km<sup>2</sup>), yielding ~7.6 relict conduit reaches  
428 per km<sup>2</sup>. This is a minimum estimate, because additional conduit remnants could occur below  
429 and beyond the margins of observed lakes. Conversely, the number of lake filling events (23  
430 over the 5 ablation seasons spanned by the imagery) shows that drainage routes commonly  
431 become blocked. Conduit blockage processes have been described by Gulley et al. (2009b),  
432 and include accumulation of icicles or floor-ice at the end of the melt season and creep  
433 closure of opposing conduit walls. The interplay between drainage events and conduit  
434 blockage maintains a dynamic population of supraglacial lakes, which contribute  
435 significantly to ablation of the glacier, through absorption of solar radiation and ice melt, and  
436 calving (Thompson et al., 2016).

437



438 The stability of lakes in the terminal zone probably reflects a combination of factors. These  
439 lakes are flanked by stable slopes of thick debris, which inhibit lake growth by melt or  
440 calving. Furthermore, the lakes are located at or close to the hydrologic base level of the  
441 glacier, determined by the terminal moraine that encircles the glacier terminus, inhibiting  
442 drainage via relict conduits.

443

#### 444 *4.4 Sub-marginal drainage*

445 *Observations:* Elevation differences between successive DEMs indicate linear zones of  
446 enhanced surface lowering along both margins of Ngozumpa Glacier, where troughs extend  
447 along the base of the bounding lateral moraines (Thompson et al., 2016; Fig. 10). The inner  
448 moraine slopes consist of unvegetated, unconsolidated till, and undergo active erosion by a  
449 range of processes including rockfall, debris flow and rotational landslipping (Benn et al.,  
450 2012; Thompson et al., 2016). Although the debris eroded from the moraine slopes is  
451 transferred downslope into the troughs, the troughs underwent surface lowering of 6 – 9 m  
452 from 2010 to 2015, with a total annual volume loss in the moraine-trough systems of  $0.4 \times$   
453  $10^6 \text{ m}^3 \text{ yr}^{-1}$  (Thompson et al., 2016). This implies that a large volume of ice, debris or both is  
454 evacuated annually from below the lateral margins of the glacier.

455

456 The lateral troughs form a series of closed basins, 12 on the west side and 22 on the east (Fig.  
457 9b). Eight of the basins in the west trough and 17 of those in the east contained a lake in  
458 2010, 4 (W) and 7 (E) of which had completely drained by 2012 or 2015. Four new lakes  
459 appeared in the eastern trough in 2012 or 2015, and 1 (W) and 7 (E) underwent partial  
460 drainage and/or refilling. Three basins on western side and one on the eastern side showed no  
461 fluctuations in lake area.

462



463 Benn et al. (2001) provided detailed descriptions of lake filling and drainage cycles in basins  
464 W-7 and W-5 (Lakes 7092 and 7093 in their terminology). In October 1998, basin W-7  
465 contained three shallow ponds, but by October 1999 the basin was occupied by a single large  
466 lake and water level had risen by ~9 m. Lake area had increased from 17,890 m<sup>2</sup> to 52,550  
467 m<sup>2</sup>, with 36% of the increase attributable to backwasting and calving of the surrounding ice  
468 cliffs. By September 2000, the lake had almost completely drained and only shallow ponds  
469 remained. Lake drainage occurred via an englacial conduit, which had been exposed by  
470 retreat of the lake margin. A lake in basin W-5 also underwent fluctuations in area and depth  
471 between 1998 and 2000, but did not completely drain during that time. Horodyskuj (2015)  
472 used time-lapse photography and a pressure transducer to document rapid lake-level  
473 fluctuations in this basin, including rises and falls of several metres within hours.

474

475 Short-term cycles of lake drainage and filling can also be demonstrated in other basins within  
476 the lateral trough systems using optical satellite imagery. Figure 11 shows a series of images  
477 of the east side of the glacier close to the junction with the E branch, where a supraglacial  
478 stream (Section 4.2) flows into a closed depression in Basin E-11 (Fig. 9b). A pond  
479 occupying the basin expanded in area between March and May 2009, but drained between  
480 June and August. In 2015 there is little evidence of the pond in January but a large pond is  
481 present in June.

482

483 *Interpretation:* Widespread, rapid subsidence along both margins of the glacier can be  
484 explained by enlargement and episodic collapse of sub-marginal conduits (Thompson et al.,  
485 2016). Potential internal ablation rates were calculated from energy losses associated with  
486 runoff and supraglacial lake drainage, and the resulting value of 0.12 to 0.13 x 10<sup>6</sup> m<sup>3</sup> yr<sup>-1</sup> is  
487 around 30% of the measured volume losses, the difference being at least partly attributable to  
488 sediment evacuation by meltwater.



489

490 The sub-marginal conduits appear to be perennial features of the glacier drainage system.  
491 Upwellings in Spillway Lake are active during the winter months, indicating that conduits  
492 transport water routed via the glacier bed in addition to summer melt- and rainwater.  
493 However, much of the lower ablation zone appears to be bypassed by the sub-marginal  
494 conduits, as evidenced by widespread water storage in supraglacial lakes and ponds (Section  
495 4.3). As noted above, water is intermittently discharged from lakes in the central part of the  
496 glacier into the lateral troughs via englacial conduits.

497

498 Cycles of lake drainage and filling in lateral basins indicate intermittent connections between  
499 surface catchments and the sub-marginal meltwater channels (Fig. 9b). In some cases,  
500 drainage events can be directly attributed to exploitation of englacial conduits (Benn et al.,  
501 2001). The hourly changes in lake level recorded by Horodyskuj (2015) cannot be explained  
502 by conduit opening and blockage, and more likely reflect short-term fluctuations in recharge  
503 from surface melt and water release from storage.

504

#### 505 *4.5 Spillway Lake*

506 *Observations:* In 2010, the area of the Spillway Lake surface catchment was 0.8 km<sup>2</sup>, of  
507 which 0.27 km<sup>2</sup> was occupied by the lake system. All of the water leaving the glacier passes  
508 through Spillway Lake, entering via portals or upwellings at or close to lake level, and  
509 leaving via a gap in the western lateral moraine ~1 km from the glacier terminus (1: Fig. 12).  
510 In 2009, conduit NG-05 (Fig. 5; Section 3.2) entered the NE corner of the lake and is  
511 interpreted as the distal part of the eastern sub-marginal conduit. A second conduit portal  
512 visible at the NW lake margin in the same year is interpreted as the efflux point of the  
513 western sub-marginal stream. The evolution of the Spillway Lake system, and its





514 implications for drainage system structure in this part of the glacier, are examined in Section  
515 5.4 below.

516

#### 517 *4.6 Summary*

518 The evidence presented above demonstrates that the drainage system of Ngozumpa Glacier  
519 comprises several linked elements: 1) the subglacial system; 2) supraglacial channels; 3) a  
520 perched lake - englacial conduit system; 4) sub-marginal conduits; and 5) the Spillway Lake  
521 system. These elements have a distinct spatial distribution (Fig. 13a). Evidence for seasonal  
522 subglacial water storage is restricted to active parts of the glacier downglacier of crevasse  
523 fields, where surface water can be routed to the bed. Supraglacial channels occur where  
524 surface catchments and discharge are large enough to allow channel incision rates to outpace  
525 surface ablation rates. Thus, perennial channels only occur where the glacier surface is not  
526 broken up by crevasse fields or into small, closed basins. Perched lakes occur where the  
527 glacier surface is broken up into closed basins, where the overall gradient of the glacier is  
528  $<3^\circ$ . The life cycle of perched lakes is governed by the location of englacial 'cut and closure'  
529 conduits and the frequency of connection and blockage events. Sub-marginal conduits occur  
530 below both flanks of the glacier, and transport water from supraglacial channels, intermittent  
531 drainage from perched lakes, and possibly the subglacial drainage system, into Spillway  
532 Lake. The lake lies at the hydrologic base level of the glacier, and its extent reflects the  
533 surface elevation of the glacier relative to the spillway through the terminal moraine.

534

#### 535 **5. Evolution of the drainage system**

536 In this Section, we present evidence for changes in drainage system structure through time,  
537 including features visible on Corona images from 1964 and 1965, speleological observations,  
538 and repeat surveys of Spillway Lake since 1999.

539



540 *5.1 Supraglacial channels*

541 In 1964, a connected supraglacial drainage stream network was present on the eastern side of  
542 the main trunk above the junction with the E branch (10 - 8 km from the terminus, 4950 m to  
543 4920 m a.s.l.) (Fig. 14a). By 2010, this part of the glacier had been broken up into basins E-7,  
544 E-8 and E-9, part of the lateral trough systems described in Section 4.4. Stream channels  
545 were no longer present, although a number of isolated elongate ponds occur close to some of  
546 the original channel locations (Fig. 14b). Sinuous depressions are visible in this area in the  
547 DEMs from 2010, 2012 and 2015 (Fig. 14). The depressions have an overall reduction in  
548 elevation to the south, but in detail they have up-and-down long profiles. In cross profile,  
549 they are U-shaped and become wider and deeper through time (Fig. 14b).

550

551 We hypothesize that the supraglacial channels became deeply incised and transitioned into  
552 cut-and-closure conduits, which continue to evacuate meltwater despite fragmentation of the  
553 surface topography. Channel incision may have been encouraged by thickening debris cover  
554 that would have reduced glacier surface lowering rates.

555

556 At the distal end of the eastern lateral trough, conduit NG-05 (Fig. 5) emerges into Spillway  
557 Lake. Passage morphology indicates that at this point the conduit formed by cut and closure  
558 (Section 3.2). Thus, there is evidence for a cut and closure origin of subsurface conduits at  
559 both ends of the eastern lateral trough. We therefore infer that the sub-marginal conduits on  
560 both sides of the glacier originated as supraglacial streams that became incised below the  
561 surface. Such a scenario would require a continuous slope along both glacier margins. We  
562 conclude that supraglacial streams occurred along both margins before development of the  
563 current irregular topography, but transition to cut-and-closure conduits allowed these  
564 drainage routes to persist after break-up of the glacier surface.

565



566 *5.2 Englacial conduits in the hummocky debris-covered zone*

567 Transition of drainages from supraglacial channels to cut-and-closure conduits appears to  
568 have been a widespread process on the glacier. The presence of sutures, planar voids and  
569 bands of sorted sediments in the ceilings and walls of conduits NG-01 - NG-05 indicate that  
570 they originated as supraglacial channels. As for the lateral channels, we infer that systems of  
571 supraglacial channels existed in the central part of the lower tongue before the glacier surface  
572 was broken up into small closed basins.

573

574 Differential surface ablation can eventually cause fragmentation and abandonment of cut-  
575 and-closure conduits, cutting off downstream reaches from former water sources. In  
576 abandoned reaches, processes of passage closure dominate over those of enlargement, and  
577 systems gradually shut down. Because cut and closure conduits are generally located close to  
578 the glacier surface, shut-down is commonly incomplete. Zones of narrow voids or sutures  
579 with infills of unfrozen sediment may persist, forming meandering lines of high permeability  
580 through otherwise impermeable glacier ice.

581

582 Reactivation will occur if a new water source becomes available, and a conduit remnant  
583 connects this source with a region of lower hydraulic potential. These conditions are met on  
584 stagnant, low-gradient glacier surfaces. Supraglacial lakes in closed basins provide both  
585 reservoirs of water and regions of elevated hydraulic potential. Drainage is highly episodic,  
586 and water may be stored in supraglacial lakes for years before passing farther down the  
587 system.

588

589 *5.4 Spillway Lake*

590 The recent history of Spillway Lake was discussed in detail by Thompson et al. (2012, 2016),  
591 and is briefly reviewed here. The present spillway through the SW side of the terminal



592 moraine has been in existence since at least 1965, when water emerged from the glacier and  
593 entered a small pond behind the lateral moraine (1: Fig. 12). In the following decades, the  
594 Spillway Lake system expanded upglacier from this point. On the Survey of Nepal map,  
595 based on aerial photographs taken in 1992, the lake has a ribbon-like form, extending NE for  
596 ~600 m from the spillway. The lake had essentially the same outline at the time of our first  
597 field survey in 1998, when water was observed to enter the lake via two subaerial portals and  
598 an upwelling point (Fig. 12; Benn et al., 2001; Thompson et al., 2012). Between 1998 and  
599 1999, several chasms and holes opened up on the glacier surface north of the western portal,  
600 and by 2001 these had evolved into linear ponds and lakes (2: Fig. 12). Between 2001 and  
601 2009, the Spillway Lake system underwent considerable expansion to the north, accompanied  
602 by upglacier migration of the portal locations (3, 4: Fig. 12).

603

604 The predominantly linear patterns of lake expansion, and the location of meltwater portals  
605 and upwellings, indicate that evolution of the Spillway Lake system was strongly  
606 preconditioned by the locations of shallow englacial conduits (a and b: Fig. 12). Conduit  
607 NG-05 (Section 3.4 and Fig. 5) and other examples exposed around the lake margins show  
608 that the drainage system consists of cut-and-closure conduits graded to lake level. This near-  
609 surface englacial conduit system provided pre-existing lines of weakness in the ice which,  
610 when opened up to the surface by internal ablation and collapse, were exploited by ice-cliff  
611 melting and calving processes.

612

613 Spillway Lake was thus established on a template provided by two englacial conduits (a & b,  
614 Fig. 12), which were confluent prior to 1992. As it expanded upglacier, Spillway Lake  
615 encroached on areas formerly occupied by perched lakes and incorporated former  
616 supraglacial basins. A recent example is Basin C-33, which forms an inlier within the  
617 Spillway Lake catchment (Figs. 9a and 12). This basin contained a perched lake in 2009 and



618 2010, but this drained prior to December 2012 and has not reformed. It is likely that this  
619 basin will become entirely subsumed within the Spillway Lake catchment in the near future,  
620 as a consequence of ice-cliff backwasting.

621

#### 622 *5.5 Changing drainage patterns on the glacier*

623 Comparison of the drainage system structure in 2010 with evidence on Corona imagery from  
624 1964 shows an upglacier expansion of the area occupied by closed depressions and perched  
625 lakes, and the formation and upglacier expansion of the base-level Spillway Lake (Fig. 13b).  
626 The widespread occurrence of cut-and-closure conduits (which originate by the incision of  
627 surface streams) provides evidence of an even earlier stage in drainage evolution, when  
628 supraglacial channels extended the full length of the glacier and closed basins were absent or  
629 rare (Fig. 13c). Such a drainage system might have existed during the Little Ice Age, and  
630 persisted into the early 20th Century.

631

632 Ngozumpa Glacier has thus responded to a prolonged period of negative mass balance with a  
633 systematic reordering of its drainage system, characterized by less efficient evacuation of  
634 meltwater and greater amounts of storage. More recent elements of the drainage system retain  
635 a memory of older elements, and processes and patterns of ablation on the glacier continue to  
636 be influenced by active and relict channels and conduits. Former supraglacial channels  
637 preconditioned the location and density of cut-and-closure conduits, which in turn  
638 precondition the formation and drainage of perched lakes and provide templates for the  
639 expansion of Spillway Lake.

640

#### 641 **6. Comparison with other glaciers**

642 Observations on other debris-covered glaciers in the Himalaya indicate that their drainage  
643 systems share many of the characteristics described in this paper. Seasonal velocity



644 fluctuations have been documented on other large glaciers in the Mount Everest region and  
645 on Lirung glacier, Nepal (Benn et al., 2012; Kraaijenbrink et al., 2016), indicating surface-to-  
646 bed drainage and variations in subglacial water storage. Perennial supraglacial channels occur  
647 in the upper ablation zones of many glaciers, in places where catchments are not fragmented  
648 by crevasse fields or irregular surface topography (Gulley et al., 2009b; Benn et al., 2012).  
649 Continuity between a supraglacial channel and an englacial cut-and-closure conduit has been  
650 observed on Khumbu Glacier, clearly demonstrating the genetic relationship between the two  
651 features (Gulley et al. 2009b). Perched lakes are widespread on Himalayan debris-covered  
652 glaciers, and evidence for repeated filling and drainage (Watson et al., 2016; Miles et al.,  
653 2017) suggest that englacial conduits may play an important role in their life cycles.  
654 However, englacial conduits have only been explored in a few glaciers (Gulley and Benn,  
655 2007; Gulley et al. 2009b; Benn et al. 2009), and much research remains to be done.  
656 Similarly, very little is known about possible sub-marginal channels in Himalayan glaciers,  
657 and our few attempts to enter these highly dynamic environments have been repulsed.

658

659 There is strong evidence on many glaciers that base-level lake growth is preconditioned by  
660 englacial conduits. For example, upglacier expansion of the proglacial lake at Tasman  
661 Glacier, New Zealand, has repeatedly echoed former chains of sink holes on the glacier  
662 surface (Kirkbride, 1993; Quincey and Glasser, 2009). Recently formed chains of ponds on  
663 the lower ablation zone of Khumbu Glacier, strongly suggests that the same process is  
664 underway on that glacier (Watson et al., 2016). The integrated picture of drainage system  
665 structure and evolution presented in this paper provides a framework for predicting what the  
666 future has in store for Khumbu Glacier and other debris-covered glaciers in the region.

667

## 668 **7. Summary and Conclusions**



669 This paper has provided the first synoptic view of the drainage system of a Himalayan debris-  
670 covered glacier, including the spatial distribution of system components, their evolution  
671 through time, and their influence on processes and patterns of ablation. Our specific  
672 conclusions are as follows.

673 1) In the upper ablation zone, seasonal variations in ice velocity indicate routing of surface  
674 meltwater to the bed via crevasses, and fluctuations in subglacial water storage.

675 2) Systems of supraglacial channels occur where the glacier surface is uninterrupted by  
676 crevasses or closed depressions, allowing efficient evacuation of surface melt.

677 3) Active sub-marginal channels are evidenced by linear zones of subsidence along both  
678 margins of the glacier, and fluctuations in surface water storage and release. These channels  
679 likely formed from supraglacial channels by a process of cut and closure, and permit long-  
680 distance transport of meltwater through the ablation zone. Transport of sediment via the  
681 lateral channels destabilizes inner moraine flanks and delivers debris to the terminal zone,  
682 where it modulates ablation processes.

683 4) In the lower ablation zone (below ~5,000 m) the glacier surface consists of numerous  
684 closed drainage basins. Meltwater in this zone typically undergoes storage in perched lakes  
685 before being evacuated via the englacial drainage system. Englacial conduits in this zone  
686 evolved from supraglacial channels by a process of cut-and-closure, and may undergo  
687 repeated cycles of abandonment and reactivation.

688 5) Enlargement of englacial conduits removes ice mass that is not captured by surface  
689 observations until conduit collapse occurs, with the implication that observations of sudden  
690 surface lowering need not reflect sudden glacier mass loss over the same time period.  
691 Subsurface processes play a governing role in creating, maintaining and shutting down  
692 exposures of ice at the glacier surface, with a major impact on spatial patterns and rates of  
693 surface mass loss.



694 6) A large lake system (Spillway Lake) is dammed behind the terminal moraine, which forms  
695 the hydrologic base level for the glacier. Since the early 1990s, Spillway Lake has expanded  
696 upglacier, exploiting weaknesses formed by englacial conduits.

697 7) As part of the glacier response to the present ongoing period of negative mass balance, the  
698 structure of the drainage system has changed through time, characterized by decreasing  
699 efficiency and greater volumes of storage. Processes and patterns of ablation on the glacier  
700 are strongly influenced by active and relict elements of the drainage system. Former  
701 supraglacial channels evolved into cut-and-closure conduits, which in turn precondition the  
702 formation and drainage of perched lakes and provide templates for the expansion of Spillway  
703 Lake. Thus drainage elements that initially formed during earlier active phases of the glacier's  
704 history continue to influence its evolution during stagnation.

705

#### 706 **Acknowledgements**

707 Funding for ST was provided by the European Commission FP7-MC-IEF grant PIEF-GA-  
708 2012-330805, and for LN by the Austrian Science Fund (FWF) Elise Richter Grant (V309).  
709 Financial support for fieldwork in 2009 was provided by the University Centre in Svalbard  
710 and a Royal Geographical Society fieldwork grant to ST. Field assistance was given by  
711 Annelie Bergström and Alison Banwell. TerraSAR-X data were kindly provided by DLR  
712 under Project HYD0178. The meteorological data were collected within the Ev-K2-CNR  
713 SHARE Project, funded by contributions from the Italian National Research Council and the  
714 Italian Ministry of Foreign Affairs, and we thank Patrick Wagnon of the IRD for collecting  
715 and releasing the 2014-2015 data used in this paper.

716

717

#### 718 **References**





- 719 Benn, D.I., Wiseman, S. and Warren, C.R. 2000. Rapid growth of a supraglacial lake,  
720 Ngozumpa Glacier, Khumbu Himal, Nepal. IAHS Publication 264 (*Symposium in*  
721 *Seattle 2000 – Debris Covered Glaciers*), 177-185.
- 722 Benn, D.I., Wiseman, S. and Hands, K., 2001. Growth and drainage of supraglacial lakes on  
723 the debris-mantled Ngozumpa Glacier, Khumbu Himal. *Journal of Glaciology*, 47, 626-  
724 638.
- 725 Benn, D.I., Kirkbride, M.P., Owen, L.A. and Brazier V. 2003. Glaciated valley landsystems.  
726 In: Evans, D.J.A. (ed.) *Glacial Landsystems*. Arnold, 372-406.
- 727 Benn, D.I., Gulley, J., Luckman, A., Adamek, A. and Glowacki, P. 2009. Englacial drainage  
728 systems formed by hydrologically driven crevasse propagation. *Journal of Glaciology*  
729 55 (191), 513-523.
- 730 Benn, D.I., Bolch, T., Dennis, K., Gulley, J., Luckman, A., Nicholson, K.L., Quincey, D.,  
731 Thompson, S. and Tuomi, R. and Wiseman, S. Response of debris-covered glaciers in  
732 the Mount Everest region to recent warming, and implications for outburst flood  
733 hazards. *Earth Science Reviews* 114, 156-174.
- 734 Bolch, T., Buchroithner, M., Pieczonka, T. and Kunert, A. 2008a. Planimetric and volumetric  
735 glacier changes in the Khumbu Himal, Nepal, since 1962 using Corona, Landsat TM  
736 and ASTER data. *Journal of Glaciology* 54 (187), 592-600.
- 737 Bolch, T., Buchroithner, M., Peters, J., Baessler, M. and Bajracharya, S. 2008b. Identification  
738 of glacier motion and potentially dangerous glacial lakes in the Everest region/Nepal  
739 using spaceborne imagery. *Natural Hazards and Earth System Science* 8, 1329-1340.
- 740 Bolch, T., Pieczonka, T. and Benn, D.I. 2011 Multi-decadal mass loss of glaciers in the  
741 Everest area (Nepal Himalaya) derived from stereo imagery. *The Cryosphere* 5, 349-  
742 358.
- 743 Clayton, L. 1964. Karst topography on stagnant glaciers. *Journal of Glaciology* 5: 107-112.



- 744 Fountain, A.G. and Walder J. 1998. Water flow through temperate glaciers. *Reviews of*  
745 *Geophysics* 36, 299-328.
- 746 Gulley, J. and Benn, D.I. 2007. Structural control of englacial drainage systems in Himalayan  
747 debris-covered glaciers. *Journal of Glaciology* 53, 399-412.
- 748 Gulley, J., Benn, D.I., Screaton, L. and Martin, J. 2009a. Englacial conduit formation and  
749 implications for subglacial recharge. *Quaternary Science Reviews* 28 (19-20), 1984-  
750 1999.
- 751 Gulley, J., Benn, D.I., Luckman, A. and Müller, D. 2009b. A cut-and-closure origin for  
752 englacial conduits on uncrevassed parts of polythermal glaciers. *Journal of Glaciology*  
753 55 (189), 66-80.
- 754 Hambrey M J, Quincey D J, Glasser N F, Reynolds J M, Richardson S J and Clemmens S  
755 2008 Sedimentological, geomorphological and dynamic context of debris-mantled  
756 glaciers, Mount Everest (Sagarmatha) region, Nepal. *Quaternary Science Reviews* 27  
757 2361–2389.
- 758 Hands, K.A. 2004. *Downwasting and supraglacial lake evolution on the debris-covered*  
759 *Ngozumpa Glacier, Khumbu Himal, Nepal*. Unpublished PhD thesis, University of St  
760 Andrews.
- 761 Hansen, O.H. 2001. Internal drainage of some subpolar glaciers on Svalbard. Unpublished  
762 MSc thesis, The University Centre in Svalbard.
- 763 Humlum O. Elberling B. Hormes A. Fjordheim K. Hansen OH. Heinemeier J. 2005. Late-  
764 Holocene glacier growth in Svalbard, documented by subglacial relict vegetation and  
765 living soil microbes. *The Holocene* 15: 396-407.
- 766 Jarosch, A.H. and Gudmundsson, M.T. 2012. A numerical model for meltwater channel  
767 evolution in glaciers. *The Cryosphere* 6, 493-503.
- 768 Kääh, A., Berthier, E., Nuth, C., Gardelle, J. and Arnaud, Y. 2012. Contrasting patterns of  
769 early twenty first century glacier mass change in the Himalayas. *Nature* 488, 495-498.s



- 770 Kirkbride, M.P. 1993. The temporal significance of transitions from melting to calving  
771 termini at glaciers in the central Southern Alps of New Zealand. *The Holocene* 3: 232-  
772 240.
- 773 Kraaijenbrink, P., Meijer, S.W., Shea, J.M., Pellicciotti, F., De Jong, S.M. and Immerzeel,  
774 W.W. 2016. Seasonal surface velocities of a Himalayan glacier derived by automated  
775 correlation of Unmanned Aerial Vehicle imagery.” *Annals of Glaciology* 57 (71): 103-  
776 13.
- 777 Krüger, J. 1994. Glacial processes, sediments, landforms, and stratigraphy in the terminus  
778 region of Myrdalsjökull, Iceland. *Folia Geographica Danica*, 21, 1-233.
- 779 Mertes, J., Thompson, S.S., Booth, A.D., Gulley, J.D. and Benn, D.I. 2016. A conceptual  
780 model of supraglacial lake formation on debris-covered glaciers based on GPR facies  
781 analysis. *Earth Surface Processes and Landforms* doi: 10.1002/esp.4068.
- 782 Miles, E. S., Pellicciotti, F., Willis, I. C., Steiner, J. F., Buri, P., & Arnold, N. S. 2015.  
783 Refined energy-balance modelling of a supraglacial pond, Langtang Khola, Nepal.  
784 *Annals of Glaciology* 57, 29-40.
- 785 Miles, E., Willis, I., Arnold, N., Steiner, J. and Pellicciotti, F. 2017. Spatial, seasonal and  
786 interannual variability of supraglacial ponds in the Langtang Valley of Nepal, 1999-  
787 2013. *Journal of Glaciology* 63 (237), 85-105.
- 788 Nakawo, M, Iwata, S., Watanabe, O. and Yoshida, M., 1986. Processes which distribute  
789 supraglacial debris on the Khumbu Glacier, Nepal Himalaya. *Annals of Glaciology* 8,  
790 129-131.
- 791 Nicholson, L.A. 2004. *Modelling melt beneath supraglacial debris: Implications for the*  
792 *climatic response of debris-covered glaciers*. PhD thesis, University of St Andrews,  
793 UK.
- 794 Nicholson, L.A. and Benn, D.I. 2006. Calculating ablation beneath a debris layer from  
795 meteorological data. *Journal of Glaciology* 52 (187), 463-470.



- 796 Nicholson, L. and Benn, D.I. 2012. Properties of natural supraglacial debris in relation to  
797 modelling sub-debris ice ablation. *Earth Surface Processes and Landforms* 38, 490-501.
- 798 Quincey, D.J. and Glasser, N.F. 2009. Morphological and ice-dynamical changes on the  
799 Tasman Glacier, New Zealand, 1990-2007. *Global and Planetary Change*, 68, 185-197.
- 800 Quincey, D.J., Lucas, R.M., Richardson, S.D., Glasser, N.F., Hambrey, M.J. and Reynolds,  
801 J.M. 2005. Optical remote sensing techniques in high-mountain environments:  
802 application to glacial hazards. *Progress in Physical Geography* 29, 475-505.
- 803 Quincey, D.J., Richardson, S.D., Luckman, A., Lucas, R.M., Reynolds, J.M., Hambrey, M.J.  
804 and Glasser, N.F. 2005. Early recognition of glacial lake hazards in the Himalaya using  
805 remote sensing datasets. *Global and Planetary Change* 56, 137-152.
- 806 Quincey, D., Luckman, A. and Benn, D.I. 2009. Quantification of Everest-region glacier  
807 velocities between 1992 and 2002 using satellite radar interferometry and feature  
808 tracking. *Journal of Glaciology* 55 (192), 596-606.
- 809 Richardson, S.D. and Reynolds, J.M. 2000. An overview of glacial hazards in the Himalayas.  
810 *Quaternary International*, 65-66, 31-47.
- 811 Sakai, A., Nakawo, M. and Fujita, K. 1998. Melt rates of ice cliffs on the Lirung Glacier,  
812 Nepal Himalaya, 1996. *Bulletin of Glacier Research* 16, 57-66.
- 813 Sakai, A., Takeuchi, N., Fujita, K. and Nakawo, M. 2000. Role of supraglacial ponds in the  
814 ablation process of a debris covered glacier in the Nepal Himalayas. IAHS Publication  
815 264 (*Symposium in Seattle 2000 – Debris Covered Glaciers*), 119-130.
- 816 Sakai, A., Nishimura, K., Kadota, T. and Takeuchi, N. 2009. Onset of calving at supraglacial  
817 lakes on debris covered glaciers of the Nepal Himalaya. *Journal of Glaciology* 55, 909-  
818 917.
- 819 Thompson, S., Benn, D.I., Dennis, K. and Luckman, A. 2012. A rapidly growing moraine  
820 dammed glacial lake on Ngozumpa Glacier, Nepal. *Geomorphology* 145-146, 1-11.



- 821 Watanabe, O., Iwata, S. and Fushimi, H. 1986. Topographic characteristics in the ablation  
822 area of the Khumbu Glacier, Nepal Himalaya. *Annals of Glaciology* 8, 177-180.
- 823 Watson, C.S., Quincey, D.J., Carrivick, J.L. and Smith, M.W., 2016. The dynamics of  
824 supraglacial ponds in the Everest region, central Himalaya. *Global and Planetary*  
825 *Change* 142, 14-27.
- 826 Wessels, R.L., Kargel, J.S. and Kieffer, H.H. 2002. ASTER measurement of supraglacial  
827 lakes in the Mount Everest region of the Himalaya. *Annals of Glaciology* 34, 399-408.
- 828 Vuichard, D. and Zimmermann, M. 1987. The 1985 catastrophic drainage of a moraine-  
829 dammed lake, Khumbu Himal, Nepal: causes and consequences. *Mountain Research*  
830 *and Development* 7, 91-110.
- 831 Yamada, T., 1998. *Glacier lake and its outburst flood in the Nepal Himalaya*. Monograph  
832 No. 1, Data Centre for Glacier Research, Japanese Society of Snow and Ice, Japan, 96  
833 pp.
- 834
- 835
- 836



837 Table 1: Satellite imagery used in the paper

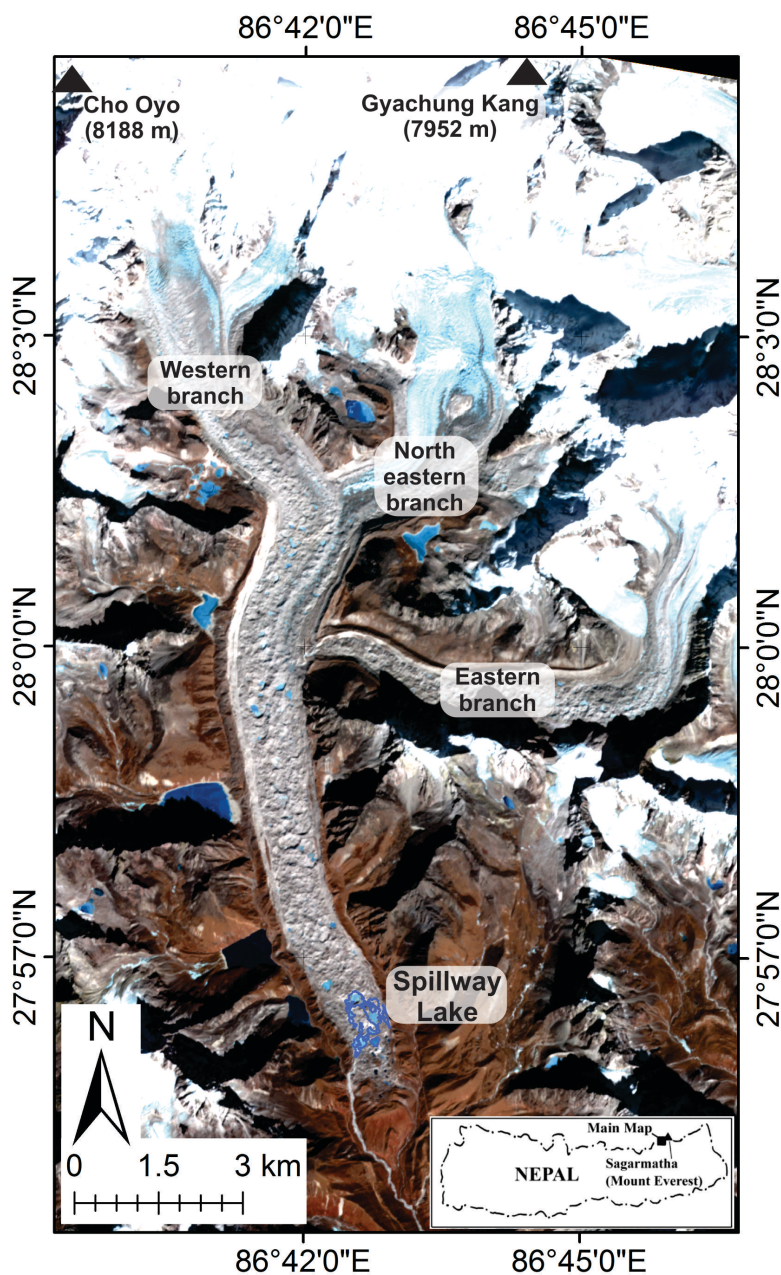
<b>Sensor</b>	<b>Product type</b>	<b>Resolution m</b>	<b>Acquisition date</b>	<b>Cloud cover (%)</b>
<b>Corona</b>	KH-4	3	04 Mar. 1965	-
<b>Landsat 5 TM</b>	Level T1	30	05 Mar. 2009	17
<b>Landsat 5 TM</b>	Level T1	30	08 May 2009	16
<b>Landsat 5 TM</b>	Level T1	30	09 Jun. 2009	28
<b>Landsat 5 TM</b>	Level T1	30	16 Aug. 2009	18
<b>GeoEye-1</b>	GeoStereo	PAN 0.46	09 Jun. 2010	3
	PAN/MSI	MSI 1.84		
<b>GeoEye-1</b>	GeoStereo	PAN 0.46	23 Dec. 2012	0
	PAN/MSI	MSI 1.84		
<b>WorldView-3</b>	GeoStereo	PAN 0.46	05 Jan. 2015	0
	PAN/MSI	MSI 1.84		

838

839

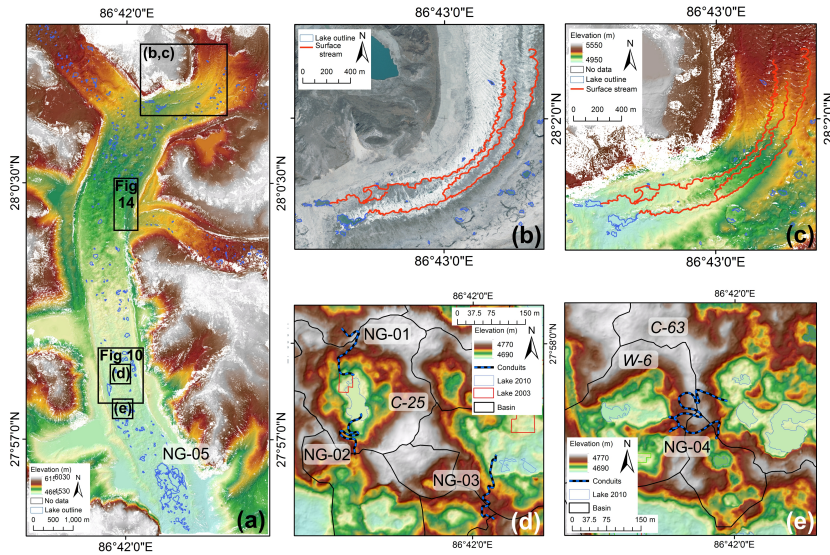
840

841



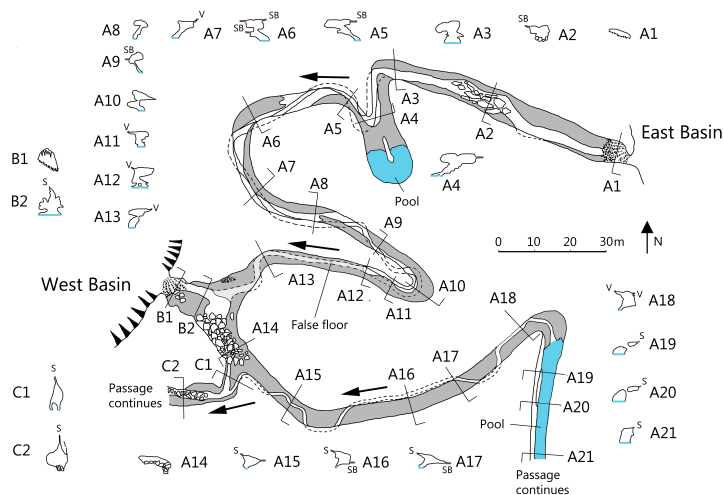
842  
843 Fig. 1: Ngozumpa Glacier, showing the location of the three branches and Spillway Lake.  
844 Image: orthorectified GeoEye-1 from December 2012.  
845





846  
 847  
 848  
 849  
 850  
 851  
 852  
 853  
 854  
 855  
 856  
 857  
 858

Fig. 2: Examples of surface topography, supraglacial meltwater channels and englacial conduit locations on Ngozumpa Glacier: a) DEM of the lower ablation zone of the glacier, showing location of panels b-e, Figs. 10 & 14, and englacial conduit NG-05; b) supraglacial channels shown on GeoEye-1 imagery from June 2010; c) the same area shown on the 2010 DEM; d) hummocky debris-covered ice showing the boundaries of closed surface basins and locations of englacial conduits NG-01 to NG-03. Considerable basin expansion occurred in the 4 ablation seasons between the conduit surveys (December 2005) and the date of the DEM (June 2010); e) hummocky debris-covered ice and location of englacial conduit NG-04 (surveyed November 2009, 7 months before the date of the DEM).

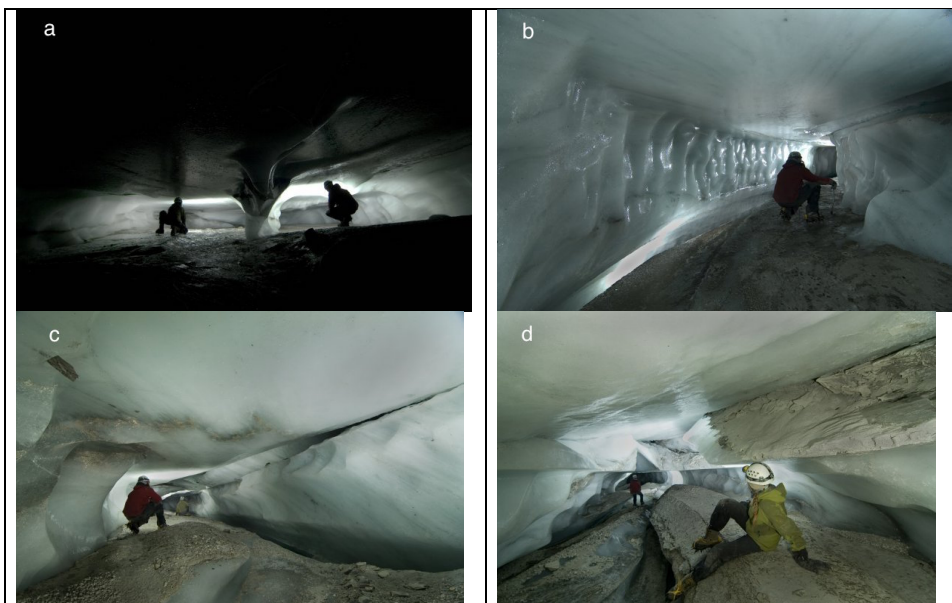


859

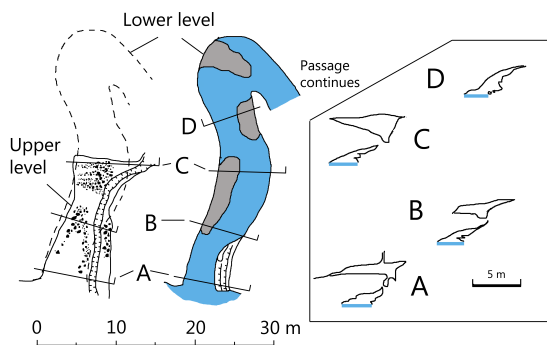




860 Fig. 3: Plan and passage cross sections, englacial conduit NG-04. SB: sediment band, S:  
 861 suture, V: voids. Grey shaded areas indicate the floor of the upper level and blue areas  
 862 indicate standing water. Arrows show the floor slope directions of the lower level.  
 863



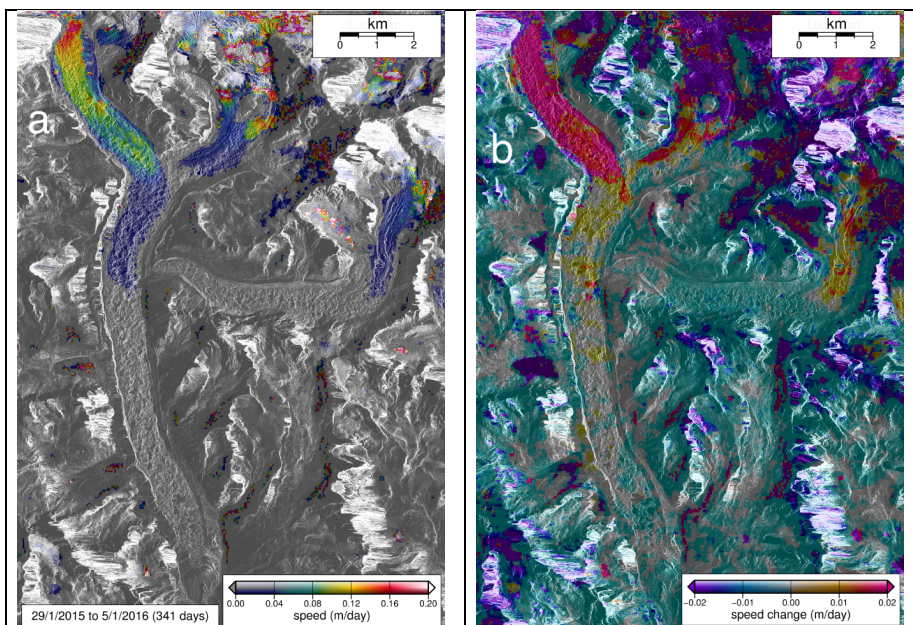
864 Fig. 4: Passage morphology in NG-04. a) Cutoff meander loop. Note inclined debris band on  
 865 back wall behind the the left-hand figure. b) The upper passage near A12, showing suture  
 866 between the right-hand wall and the ceiling, and the incised lower passage on the left. c) The  
 867 upper passage near A7, with a void and suture between the right-hand wall and the ceiling. d)  
 868 The upper passage near A6, showing a band of bedded sand filling a sub-horizontal suture  
 869 above the foreground figure.  
 870  
 871



872  
 873 Fig. 5: Plan and passage cross-sections, conduit NG-05. 'Upper-' and Lower level' refer to the  
 874 two floor levels indicated in cross-sections A-C. For location see Figure 12.  
 875

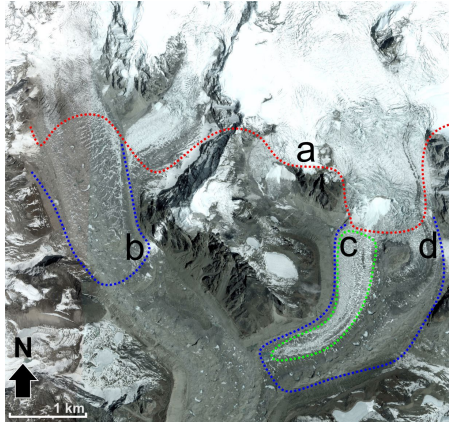


876 Fig. 6: a) The entrance of NG-05 on the NW margin of Spillway Lake; b) NG-01: debris-  
877 filled canyon suture at the upper level of the cave; c) NG-01: flat-floored mid level of the  
878 cave. Note canyon suture above and incised lower level crossing foreground from left to  
879 right; d) NG-02: Tubular upper passage with canyon suture in the roof.  
880

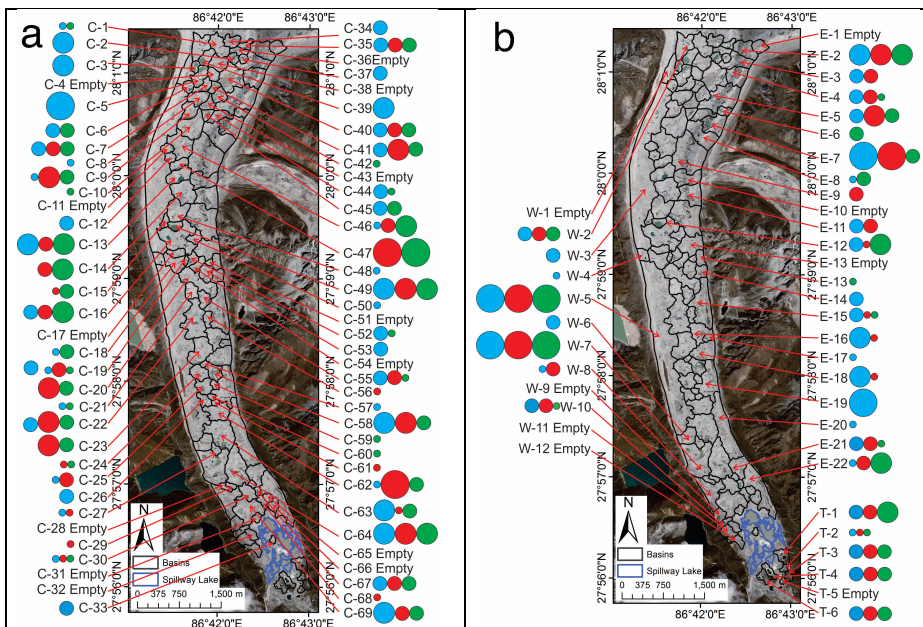


881 Fig. 7: Surface velocities derived from TerraSAR-X data: a) mean daily velocity for the  
882 'annual' period 29 Jan 2015 to 5 Jan 2016; b) mean daily velocities for 29 Jan 2015 to 5 Jan  
883 2016 minus mean daily velocities for 19 Sept 2014 to 18 Jan 2015, indicating minimum  
884 summer speed-up of the glacier.  
885  
886

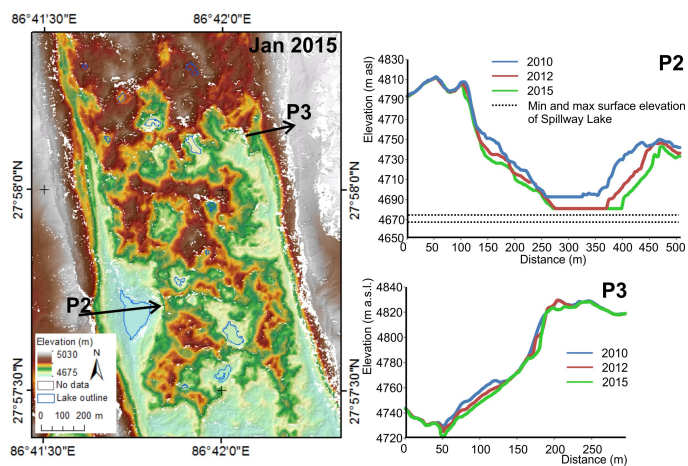




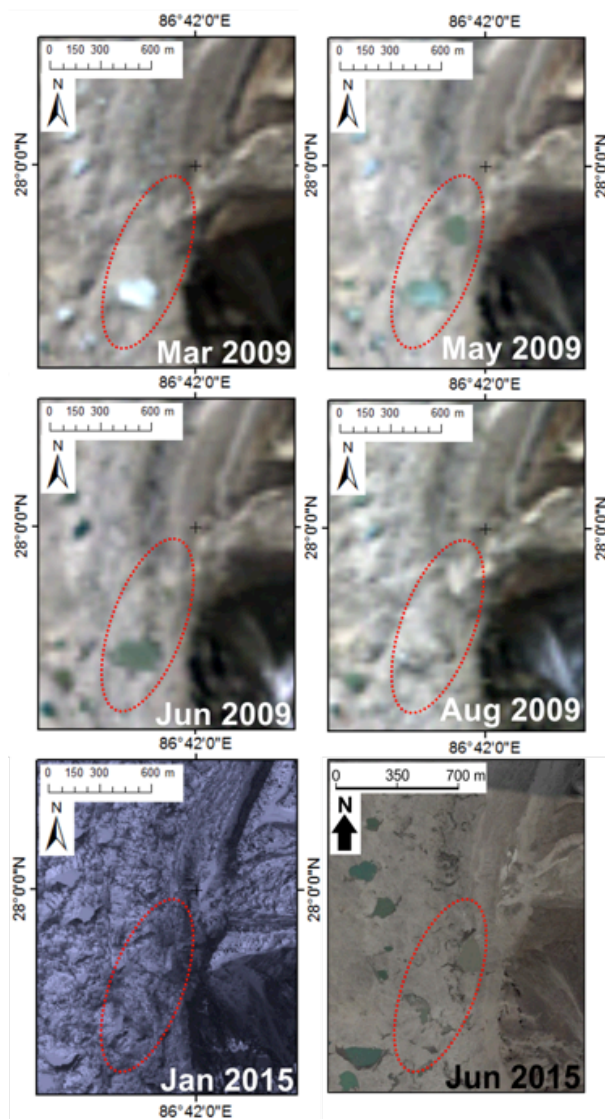
887  
 888 Fig. 8: The location of crevasse fields on the W and NE branches of Ngozumpa Glacier (a)  
 889 and areas where supraglacial channels occur on debris-covered (b, d) and clean (c) ice. Image  
 890 source: Google Earth  
 891  
 892  
 893  
 894  
 895  
 896  
 897



898  
 899 Fig. 9: Surface drainage basins and lake area changes: a) the central part of the glacier, and b)  
 900 the lateral margins and terminal zone. Lake areas are shown for 2010 (blue), 2012 (red) and  
 901 2015 (green), in four categories:  $<1000 \text{ m}^2$  (small circles),  $1000\text{-}5000 \text{ m}^2$  (medium circles),  
 902  $5000\text{-}10000 \text{ m}^2$  (large circles) and  $>10000 \text{ m}^2$  (largest circles).  
 903

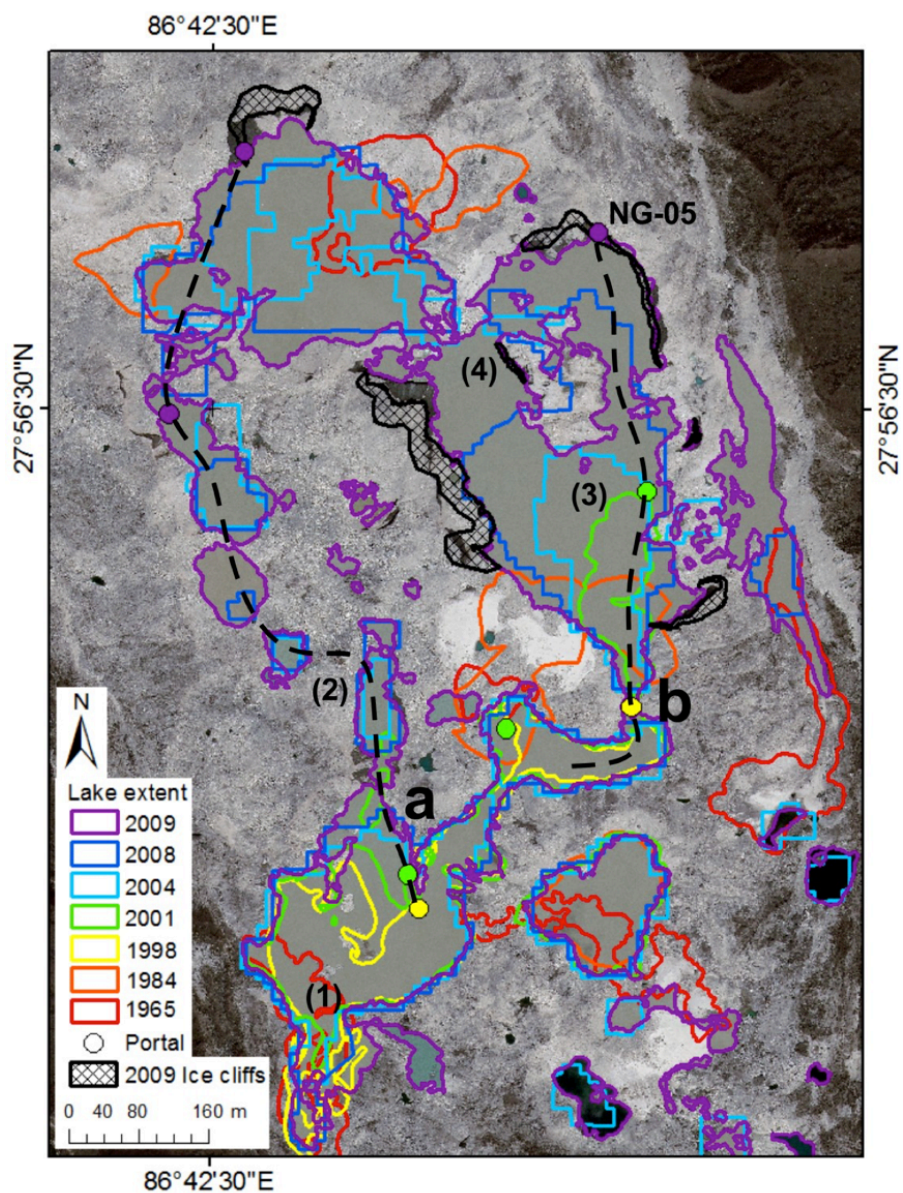


904  
905 Fig. 10: Extract from the 2010 DEM and selected cross profiles in 2010, 2012 and 2015  
906 showing lateral troughs, subsidence of trough floors and erosion of moraine slopes. Location  
907 of the map is shown in Fig. 2.

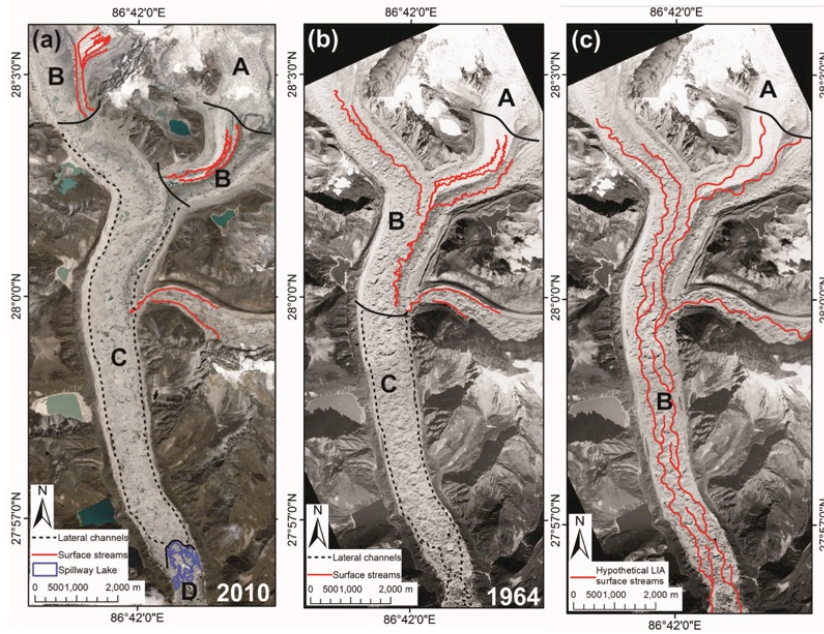


908  
909 Fig. 11: Changing lake extent in Basin E-11, showing evidence of filling and drainage cycles,  
910 on Landsat 5 TM (2009), WorldView-3 (Jan 2015) and (Jun 2015) imagery.

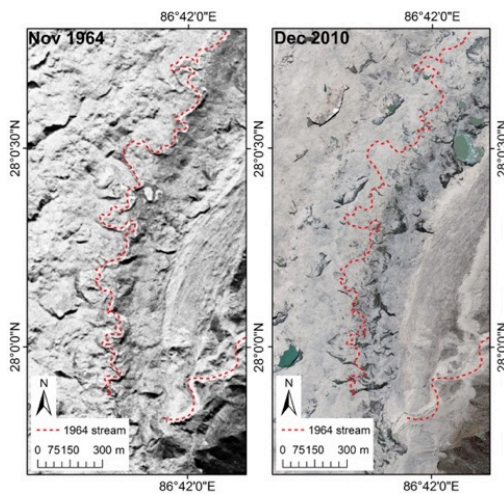




911  
912 Fig. 12: Spillway Lake, 1965-2009, showing the position of meltwater portals and upwellings  
913 and the inferred location of englacial conduits (dashed lines). Background image: GeoEye-1  
914 from June 2010.



915  
 916 Fig. 13: Zonation of the drainage system in 2010 and 1964, and a hypothetical drainage  
 917 system at the Little Ice Age maximum. A: crevasse fields; B: supraglacial channels; C: closed  
 918 surface basins with perched lakes; D: Spillway lake. Dashed lines indicate the positions of  
 919 sub-marginal conduits.  
 920



921  
 922  
 923 Fig. 14: Eastern margin of the main trunk upglacier from its confluence with the E branch,  
 924 showing supraglacial channels (Corona imagery from 1964) and hummocky surface  
 925 topography (GeoEye-1 imagery from 2010). For location of area see Fig. 2.  
 926  
 927